L 3/8

Yield Surfaces for Perforated Sheets

M. König
*Universität Stuttgart, Institut für Statik und Dynamik der Luft- und Raumfahrtkontruktionen,
Pfaffenwaldring 27, D-7000 Stuttgart 80, Germany*

Abstract

The presentation shows how elasto-plastic constitutive relations, i.e. effective constants, initial and subsequent yield surfaces and a flow rule for the "equivalent solid material" as required for the stress analysis of perforated sheets, can be obtained by performing numerical experiments with a unit cell, cut out of the perforated sheet. This is done by idealizing the unit cell by finite elements and applying specific load conditions.

The results given in the presentation are valid for plane stress conditions, an equilateral triangular penetration pattern and an elastic-perfectly plastic basic material. However, the method of approach could also be applied when the basic material exhibits strain hardening. In addition, the method could be applied for generalized plane strain conditions or plate bending conditions and for penetration patterns other than the equilateral triangular pattern by choosing a unit cell, satisfying the symmetry conditions of the pattern considered.

1. Method of Approach

The problem considered is represented in figure 1. We assume that the pitch of the penetration pattern is small compared with the region of constant global stresses σ_x , σ_y , σ_{xy} . Then the criterion indicating first local yielding in the perforated sheet can be expressed as a function of the global stress state . This function represents the initial yield condition of the "equivalent solid material". This yield condition can graphically be represented by a closed curve in a σ_1, σ_2 -diagram with σ_1 , σ_2 being the principal stresses of the global stress state σ_x , σ_y , σ_{xy} . All purely elastic stress states are found within the region enclosed by the curve, which represents the initial yield surface of the "equivalent solid material", whereas elasto-plastic stress states are reached by penetrating the yield surface. Due to the fact that the elasto-plastic behaviour of the perforated sheet is anisotropic, the initial yield surface changes with changing principal stress direction. Loading beyond the initial yield surface leads to a series of subsequent yield surfaces.

The method used for obtaining the yield surfaces, as well as the elastic stress, strain relation and the flow rule for the "equivalent solid material", consists in cutting out of the perforated sheet a representative unit cell and performing numerical experiments with this unit cell, employing the finite element method.

Due to the symmetry conditions of the largely extended sheet under constant global stress, the part surrounded by the thick line in figure 1 can be used as unit cell for the numerical experiments. Special attention has to be paid to the fact that the local stresses caused by the symmetric loading σ_x and σ_y have the same sign at both sides of the symmetry lines $A-A$ and $C-C$, whereas the stresses caused by σ_{xy} have the opposite sign.

Figure 2 shows a typical finite element model as used for evaluating the symmetrical loading conditions, and figure 3 shows the corresponding model for the antisymmetrical loading condition.

2. Discussion of Results

For the results presented, an elastic-perfectly plastic basic material with yield limit σ_{0F}, obeying the v. Mises yield condition and the associated (Prandtl-Reuss) flow rule has been assumed. Young's modulus $E_0 = 210\,000\ N/mm^2$ and Poisson's ratio $\nu_0 = 0.3$ have been chosen, which corresponds to steel. All results are valid for a ligament efficiency of 0.2.

Figure 4 shows initial yield surfaces for the "equivalent solid material". The parameter φ is the angle between the principal stress direction and the x-axis in figure 1. Up to the first yield, the behaviour is linerly elastic. Hence, the resulting local stress distribution for a given angle φ and a chosen combination of σ_1 and σ_2 can be obtained (after transforming σ_1 and σ_2 into σ_x, σ_y, σ_{xy}) by superposition of a symmetrical and an antisymmetrical loading case. By comparing the superposed local stresses with the yield limit of the basic material, the initial yield limit of the "equivalent solid material" is obtained. Evaluating the relation between global strains and global stresses in the elastic range yields isotropic behaviour with $G = E/(2(1+\nu))$, which is in agreement with [1]. For a ligament efficiency of 0.2 and $\nu_0 = 0.3$ there result $E/E_0 = 0.1462$ and $\nu = 0.4888$.

An approximation for the initial yield surfaces, which is independent of the principal stress direction and, hence, isotropical in the plane of the sheet, is shown graphically in figure 5. This approximation is obtained by specializing Hill's anisotropic yield condition [2] for the case of a transversely isotropic material [3].

Figure 6 shows the uniaxial stress, strain-diagram of the "equivalent solid material", obtained by numerical experiments with σ_x-loading, according to figure 1. Loading beyond the initial yield point exhibits a strain hardening region and finally a region with unlimited yielding. This es expected since the basic material is elastic-perfectly plastic. The unloading experiments show an ideal Bauschinger effect. Stressing in the opposite direction finally ends at the stress level of unlimited yielding. Hence, in the biaxial case, we can expect a limit yield surface which is independent of the load history.

In figure 7, subsequent yield surfaces in the hardening region of the "equivalent solid material" are given, as obtained after prestressing in different directions. These yield surfaces have been obtained using a special procedure, described in [4].

Figure 8 shows the initial yield surface, subsequent yield surfaces and the limit yield surface for the "equivalent solid material" in the case of monotonic loading. The subsequent yield surfaces have been obtained by postulating work hardening behaviour [5]. This postulate and the normality rule for plastic flow have been confirmed by chosing in addition to the original "radial" loading passes, loading passes that cross the original passes. Hence, the associated flow rule can be adopted. Due to the symmetry of the "equivalent solid material", which is a result of the symmetry of the penetration pattern, the approximation proposed for the initial yield surfaces can be adopted also for the subsequent yield surfaces and for the limit yield surface.

References

[1] SLOT, T., "Stress Analysis of Thick Perforated Plates", Technomic Publishing Co., Inc., 265 W. State, Westport, CT 06880 (1972).

[2] HILL, R., "The Mathematical Theory of Plasticity", Oxford University Press, London (1950).

[3] BACKOFEN, W.A., HOSFORD JR., W.F., BURKE, J.J., "Texture Hardening", Trans. ASM 55 (1962), pp. 264-267.

[4] KÖNIG, M., "Zum elastisch-plastischen Verhalten der in einem gleichförmigen Dreiecks-Lochmuster perforierten Scheibe unter ebenem Spannungszustand", Dr.-Ing. Thesis, University of Stuttgart (1983).

[5] BLAND, D.R., "The Associated Flow Rule of Plasticity", J. of the Mechanics and Physics of Solids 6 (1957), pp. 71-78.

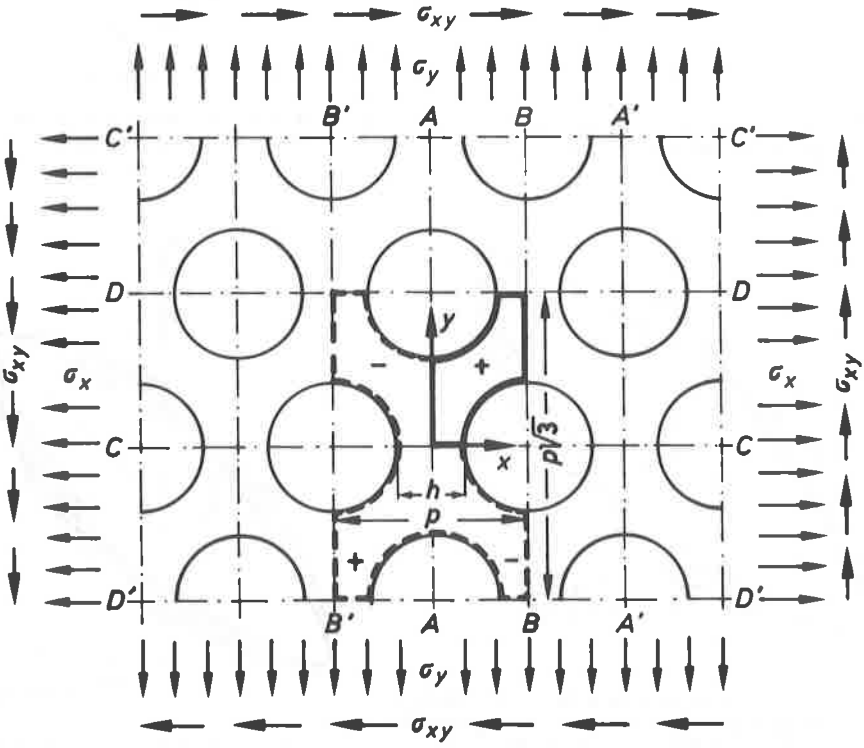

Fig. 1: Problem considered: Perforated plate with equilateral triangular penetration pattern under plane stress. (Ligament efficiency: h/p)

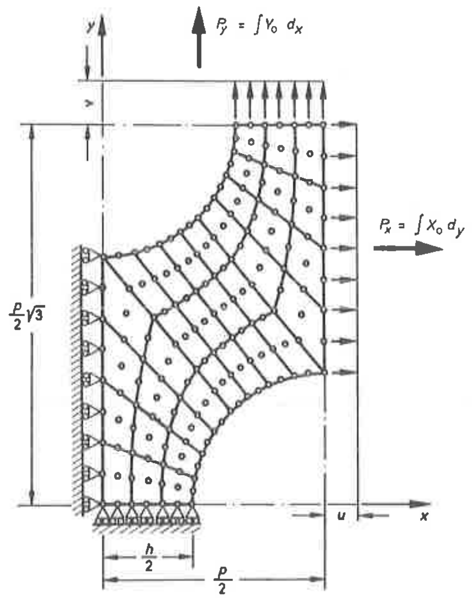

Thickness : 1

$$\sigma_x = \frac{P_x}{(p/2)\sqrt{3}} \qquad \sigma_y = \frac{P_y}{p/2}$$

$$\gamma_x = \frac{u}{p/2} \qquad \gamma_y = \frac{v}{(p/2)\sqrt{3}}$$

Fig. 2: Typical finite element model for evaluation of symmetrical loading conditions.

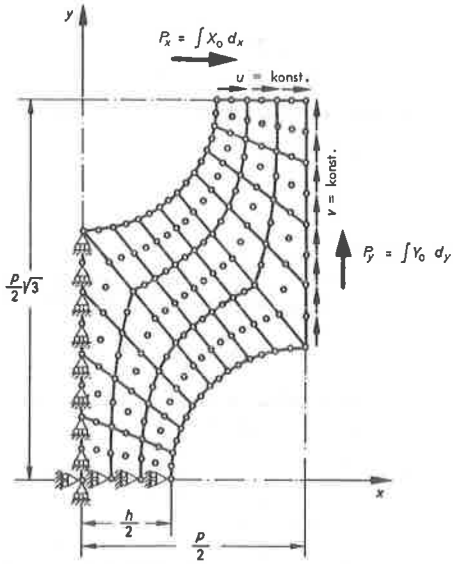

Thickness : 1

$$\sigma_{xy} = \frac{P_y}{(p/2)\sqrt{3}} = \frac{P_x}{p/2}$$

$$\gamma_{xy} = \frac{v}{p/2} + \frac{u}{(p/2)\sqrt{3}}$$

(Specific cases : $u = 0$ and $v = 0$)

Fig. 3: Typical finite element model for evaluation of the antisymmetrical loading condition.

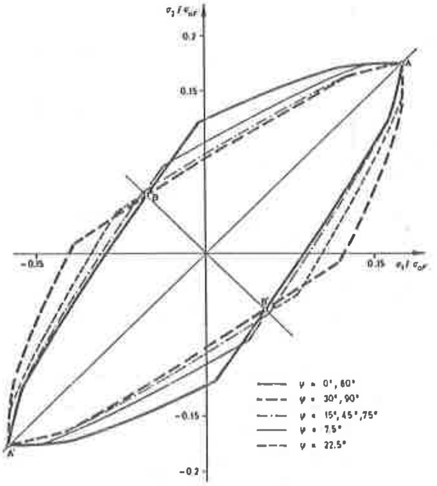

Fig. 4: Initial yield surfaces for different orientation of the principal stress direction with respect to the perforation pattern. (Ligament efficiency 0.2, φ : angle between σ_1-direction and x-axis in Fig. 1.)

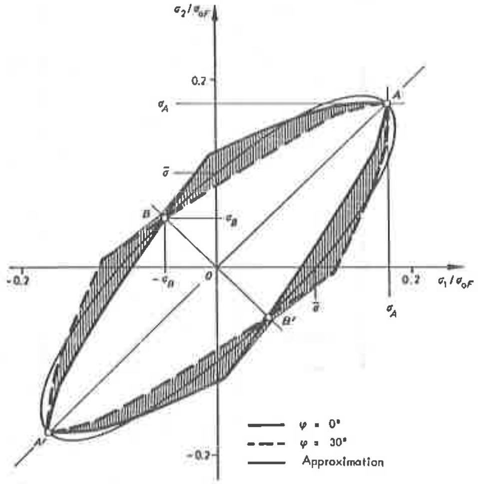

Fig. 5: Approximation proposal for initial, subsequent and limit yield surfaces in the case of monotonic loading.

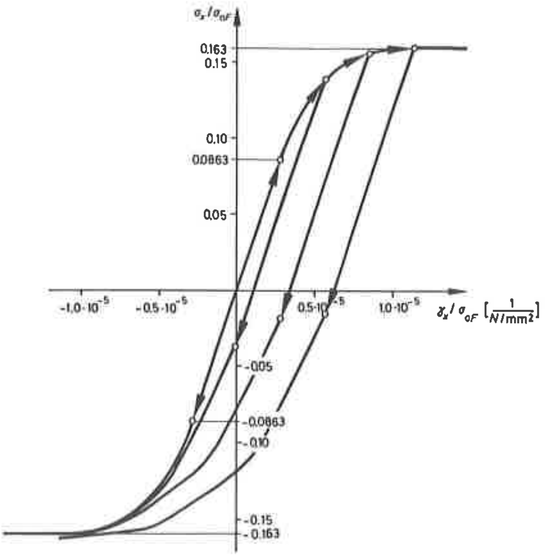

Fig. 6: Uniaxial stress-strain diagram of the "equivalent solid material" for σ_x -loading. (Ligament efficiency 0.2.)

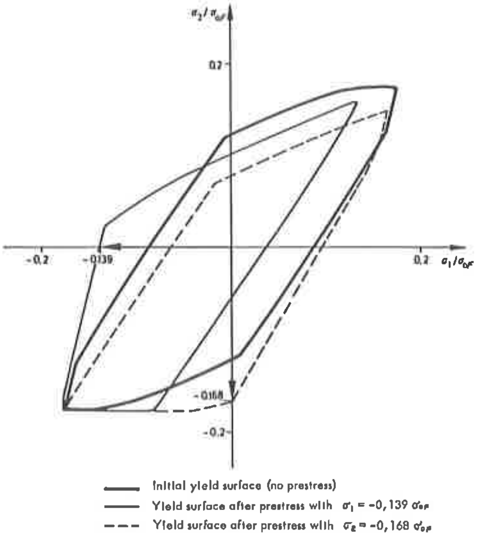

Fig. 7: Subsequent yield surfaces after prestress in different directions. (Ligament efficiency 0.2, $\varphi = 0°$.)

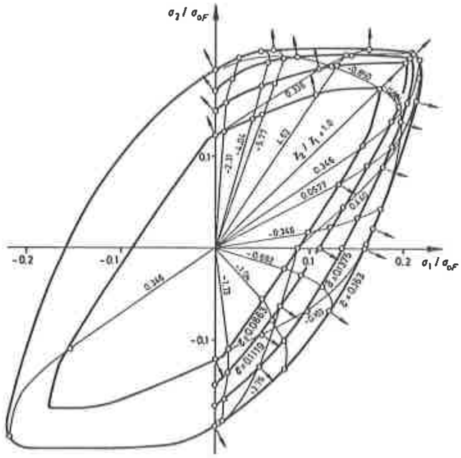

Fig. 8: Initial, subsequent and limit yield surfaces in the case of monotonic loading. (Ligament efficiency 0.2, $\varphi = 0°$.)